Molecular dynamics study of a supercooled softsphere fluid

Jacques G. Amar and Raymond D. Mountain

Citation: The Journal of Chemical Physics **86**, 2236 (1987); doi: 10.1063/1.452122
View online: http://dx.doi.org/10.1063/1.452122
View Table of Contents: http://scitation.aip.org/content/aip/journal/jcp/86/4?ver=pdfcov
Published by the AIP Publishing

Molecular dynamics study of a supercooled soft-sphere fluid[a)]

Jacques G. Amar[b)] and Raymond D. Mountain
Thermophysics Division, National Bureau of Standards, Gaithersburg, Maryland 20899

(Received 30 September 1986; accepted 31 October 1986)

Results obtained from equilibrium molecular dynamics simulations (performed on a 1000-particle system) for a soft-sphere fluid in the supercooled region are presented. The hydrodynamic length l_t corresponding to the range of dynamical correlations in the transverse current is found to increase rapidly as the amount of supercooling increases. The shear viscosity and bulk viscosity are also found to increase rapidly in the supercooled region, due to the increasing contribution of the tails of the corresponding correlation functions. While the bond-orientational order parameters Q_6 and Q_8 do not increase significantly, the lifetimes of the corresponding time correlation functions also increase rapidly in the supercooled region.

I. INTRODUCTION

When a liquid is carefully cooled below the freezing point, a thermodynamically metastable fluid, referred to as a supercooled liquid, is produced. In this paper we report the results of a molecular dynamics study of the supercooled liquid state for a simple model system. This work was undertaken in part to study how transverse–current correlations in the supercooled liquid differ from those correlations in the normal, thermodynamically stable liquid. The spatial extent of these correlations had previously been found to grow significantly in the supercooled region for a model of liquid rubidium.[1] Here, we find that the growth of the transverse–current correlations is not simply a consequence of the relatively soft repulsion of the rubidium effective pair potential, but appears in fact to be a more general feature of the supercooled liquid state.

The model used in the present study is that of softly repelling spheres which interact via an inverse-twelfth power potential.[2] The equation of state of this system has been mapped out by several earlier studies,[2–4] and the freezing point and the "glass" transition point[5] have been reliably determined. In addition, although a number of equilibrium and nonequilibrium molecular dynamics simulations have been made of the transport properties of the inverse-twelfth power system,[6–8] there have been no systematic studies of their behavior in the supercooled region. These facts make the inverse-twelfth power system an attractive one for model studies of the type discussed here.

In addition to studying transverse–current correlations, we have also examined a number of other properties of this system including the thermal conductivity and shear and bulk viscosities as well as the time correlation functions associated with these transport properties. We also present results for the behavior of the time correlation functions associated with the Q_6 and Q_8 bond-orientational order parameters.[9]

Before discussing them in more detail, we give our other results in brief here: We find for the shear viscosity, a relatively rapid increase in the supercooled region, due to a relatively sharp increase in the length of the tail of the associated time correlation function as a function of increasing reduced density ρ^*. As already mentioned, a corresponding increase in the hydrodynamic length l_t associated with the range of dynamical correlations was also noted as the degree of supercooling increased. Similarly, we note a fairly abrupt change in the rate of increase of the bulk viscosity (with increasing ρ^*) in the supercooled region. This change also corresponds to a rapid increase in the length of the tail of the associated correlation function. While the Q_6 order parameter was observed to increase slightly in the supercooled region, in contrast to Q_8 which stayed the same, the lifetimes for both associated time correlation functions were observed to increase significantly in the supercooled region. In contrast to this, we find that the correlation functions associated with self-diffusion, the thermal conductivity, and the density–density correlation function did *not* exhibit the same rapid increase in their lifetimes. Thus, we find, in general that those properties associated with collective rearrangements such as "shear" are *enhanced* in the supercooled region (due to the slowing down in particle motions) while other properties, such as the thermal conductivity, are more-or-less smoothly continued from the equilibrium region into the supercooled liquid region. These and other results are discussed in more detail in the following sections.

II. MOLECULAR-DYNAMICS CALCULATION

Our system consisted of 1000 particles in a cube of size $L = 9.5448\ \sigma$ (density $\rho = N/V = 1.15\ \sigma^{-3}$) interacting with a repulsive interaction [$V(r) = \epsilon(\sigma/r)^{12}$] with periodic boundary conditions and the minimum image convention employed throughout. The potential was truncated at $r = 1.5\ \sigma$ [$V(r) = 0$ for $r \geqslant 1.5\ \sigma$]. The equations of motion were integrated using the Beeman algorithm,[10] with the units of length, energy, and time, respectively, taken to be σ, ϵ, and $\tau = (m\sigma^2/\epsilon)^{1/2}$, where m is the mass of a particle. From the well-known scaling properties of the $1/r^{12}$ potential all thermodynamic quantities are functions only of one variable—the reduced density $\rho^* = \rho\sigma^3/(kT/\epsilon)^{1/4}$. It has been previously determined that $\rho^* \approx 1.15$ is the thermodynamic freezing reduced density for the $1/r^{12}$ potential.[3] The system was studied from $\rho^* = 1.0$ ($T^* = kT/\epsilon = 1.74$, equilibrium liquid) to $\rho^* = 1.32$ ($T^* = 0.575$) where the onset

[a)] Contribution of the National Bureau of Standards, not subject to copyright.
[b)] National Research Council Postdoctoral Fellow.

of homogeneous nucleation to an fcc crystallite was observed. A time step of $\Delta t = 0.005\ \tau$ was employed in these calculations except for the highest densities ($\rho^* \geqslant 1.30$) for which a time step of $\Delta t = 0.01$ was used. We note that the number of particles in our system is not consistent with the formation of a single fcc crystal due to periodic boundary conditions. However, this did not appear to prevent the onset of crystallization as determined by examining the pair-correlation function.[11]

In order to go from $\rho^* = 1.0$ into the supercooled region, the system was cooled at constant density from the initial starting state. This was done by rescaling the velocities at the rate of 0.002% per time step. The system was then equilibrated for at least 20 000 steps before data were taken. The shear viscosity (η), bulk viscosity (η_B), and thermal conductivity (λ_E) were calculated—using the Green–Kubo formulas[12–14]—from the corresponding current–current correlation functions:

$$\eta = \int_0^\infty dt\, C_s(t), \tag{1}$$

where

$$C_s(t) = (1/3VkT)\{\langle J_{xy}(0)J_{xy}(t)\rangle + \text{circ. perm.}\}$$

and

$$J_{xy} = \sum_{i=1}^{N} [\,(x_i F_{yi} + v_{xi}p_{yi})\,],$$

where x_i is the x position of particle i, F_{yi} is the force in the y direction (on particle i), v_{xi} the x component of the velocity of the ith particle, p_{xi} the x component of momentum of the ith particle, and N is the number of particles:

$$\eta_B = \int_0^\infty dt\, C_B(t), \tag{2}$$

where

$$C_B(t) = (V/3kT)\langle \Delta P_x(0)\Delta P_x(t) + \text{circ. perm.}\rangle$$

with

$$\Delta P_x = P_x - \langle P_x\rangle$$

and

$$P_x = (1/V)\sum_{i=1}^{N}(x_i F_{xi} + v_{xi}p_{xi}),$$

$$\lambda_E = \int_0^\infty dt\, C_E(t), \tag{3}$$

where

$$C_E(t) = (1/3VkT^2)\langle J_{Ex}(0)J_{Ex}(t) + \text{circ. perm.}\rangle,$$

where

$$J_{Ex} = \left\{\left[\sum_{i=1}^{N} mv_i^2/2 + \sum_{i=1}^{N}\sum_{j\neq i}(1/2)V(r_{ij})\right]v_{xi} - \sum_{i=1}^{N}\sum_{j\neq i}\frac{\partial V(r_{ij})}{\partial x_{ij}}(1/2)(\mathbf{r}_{ij}\cdot\mathbf{v}_i)\right\}.$$

The correlation functions were calculated out to $t = 6\tau$ using each step as a different time origin in order to maximize the statistics. In addition, the transverse–current correlation function was also calculated (see below) as well as the correlation functions $G_6(t) = \langle Q_6(0)Q_6(t)\rangle$ and $G_8(t) = \langle Q_8(0)Q_8(t)\rangle$. Other quantities which were routinely measured as part of the simulation included the pressure, the energy, the specific heat, the adiabatic compressibility, and the pair-correlation function $g(r)$. No unusual behavior was observed for these in the supercooled region. The coefficient of diffusion D was also measured by routinely monitoring the mean square displacement of each particle. Our results for D were essentially consistent with previous results tabulated by Cape and Woodcock[5] over a somewhat wider range of ρ^* and so we do not present them here.

The density–density correlation function $S(k_n,t) = \langle N(k_n,0)\, N(-k_n,t)\rangle$ was also calculated for $k_n = 2\pi n/L$ $n = 1, 10$ where

$$N(k,t) = \sum_{i=1}^{N} \exp[i\,\mathbf{k}\cdot\mathbf{r}_i(t)]$$

and the wave vectors $\mathbf{k}$ were taken along the x, y, and z edges of the cube. No significant change in the time dependence of the density–density correlation function for small values of k was seen in the supercooled region.

Runs were typically of the order of 115 000 time steps after equilibration although a few runs of 200 000 steps were also performed. Although the data for the correlation functions were somewhat noisy (especially for the longer times) we believe that they still accurately display the trends which would be observed had we obtained much larger statistics. Because of this our results are somewhat qualitative.

III. RESULTS

A. Shear viscosity

Figure 1 shows the increase in the reduced (dimensionless) shear viscosity[15] ($\eta^* = \eta/\epsilon\tau\sigma^5\rho^{(8/3)}$) with increasing ρ^* as the liquid is supercooled. Since the initial value of the

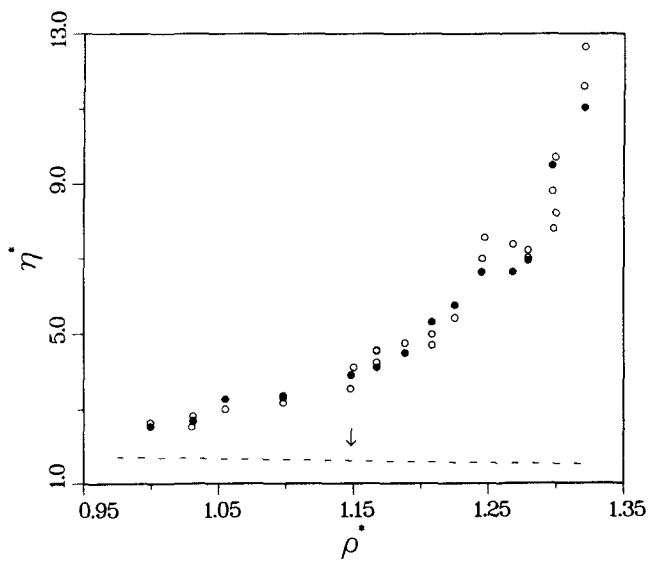

FIG. 1. Plot of η^* as a function of ρ^* in and near the supercooled region. The open circles correspond to results obtained using Eq. (1), while the black dots correspond to values extrapolated from $\eta^*(k)$ (in the limit k goes to zero) as obtained from the transverse–current correlation function [Eq. (6)]. The arrow indicates the reduced density at freezing $\rho^* \simeq 1.15$. (The Enskog values are indicated by the dashed line.)

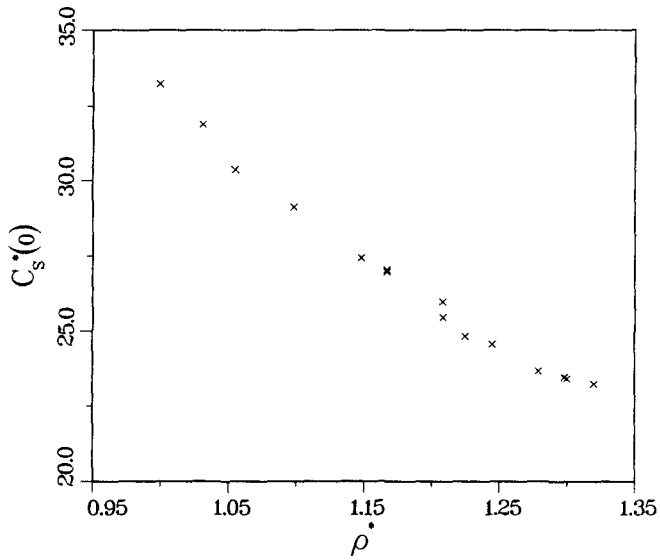

FIG. 2. Plot of $C_s^*(0)$ vs ρ^* showing the monotonic decrease of $C_s^*(0)$ with increasing ρ^*.

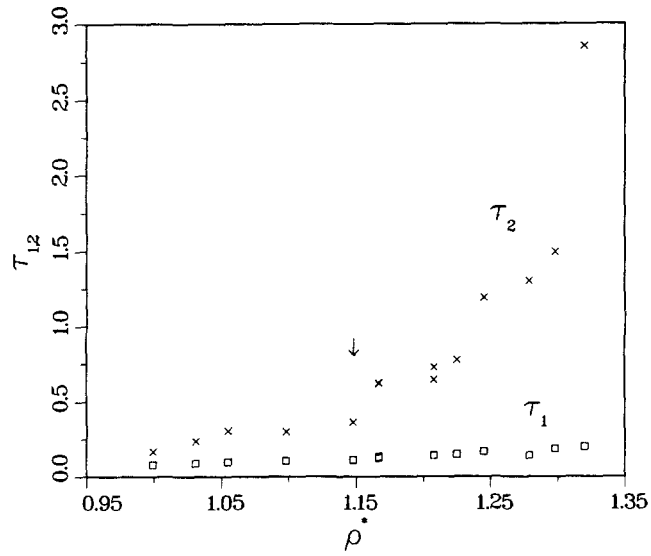

FIG. 4. Plot of short (τ_1) and long (τ_2) relaxation times characterizing the correlation function $C_s^*(t)$ as a function ρ^*. Again the arrow indicates limit of supercooled region.

correlation function $C_s^*(t)$ [$C_s^*(t) \equiv C_s(t)/\epsilon\tau^2\sigma^5\rho^{(8/3)}$] decreases as ρ^* increases (see Fig. 2), this increase in η^* is clearly due to the rapid increase of the "tail" of the correlation function $C_s^*(t)$. Figure 3 shows this increase graphically as well as the decrease in the initial value $C_s^*(0)$. The statistical error in our values of η^* increases in the supercooled region due to increased correlation times and the resulting decrease in the number of *independent* time origins over the course of a run from which to calculate the corresponding time correlation function.

In an attempt to characterize the behavior of the correlation function $C_s^*(t)$ in the supercooled region, we performed a fit of the correlation function $C_s^*(t)$ to a sum of two exponentials, one characterizing the short-time decay of $C_s^*(t)$ and the other characterizing the longer time behavior, via the expression

$$C_s^*(t) = C_s^*(0)[(1-\alpha)e^{-t/\tau_1} + \alpha e^{-t/\tau_2}].$$

This gave a fairly good fit at least up to the longer times where statistical noise became a problem. We note (see Fig. 4) that while τ_1 and τ_2 do not change much for $\rho^* < 1.15$, in the supercooled region τ_2 increases appreciably, while τ_1 remains virtually constant. Thus, the long-time behavior is clearly enhanced in the supercooled region.

We note (see Fig. 5) that the reduced viscosity $\tilde{\eta}^*$ as defined by Hiwatari *et al.*[6] ($\tilde{\eta}^* = \eta^* \cdot \rho^{*(8/3)}$) satisfies

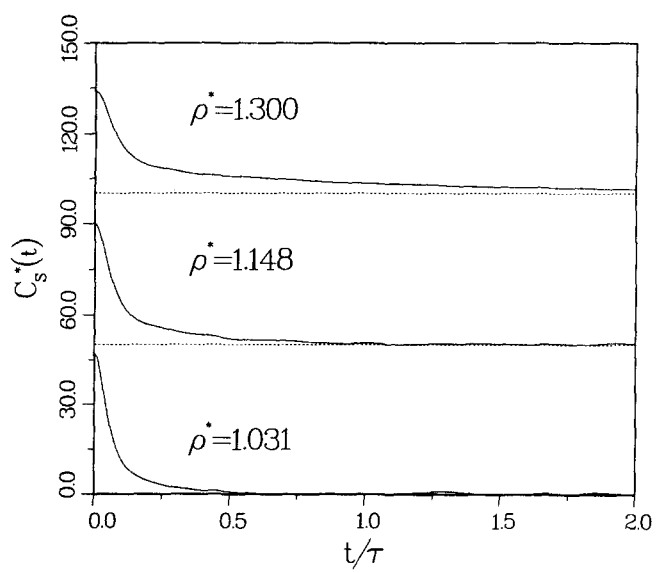

FIG. 3. The current–current correlation function $C_s^*(t)$ for three different values of ρ^*: $\rho^* = 1.031$ corresponds to equilibrium liquid ($T > T_f$), $\rho^* = 1.148$ corresponds to just below the reduced density at freezing, while $\rho^* = 1.3$ corresponds to severely *supercooled*. (For clarity, correlation functions for $\rho^* = 1.148$ and 1.3 are shifted upward in the y direction by 50 and 100 units, respectively.)

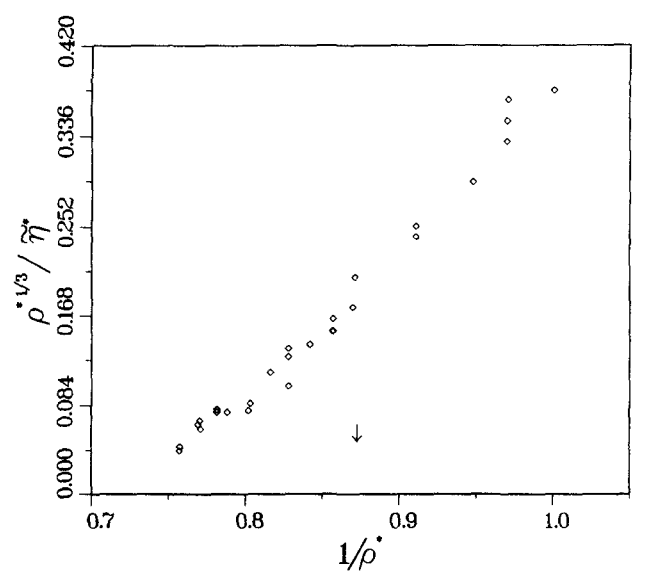

FIG. 5. Plot of $\rho^{*1/3}/\tilde{\eta}^*$ as a function of reduced volume $V^* = 1/\rho^*$. (Vertical arrow indicates limit of supercooled.)

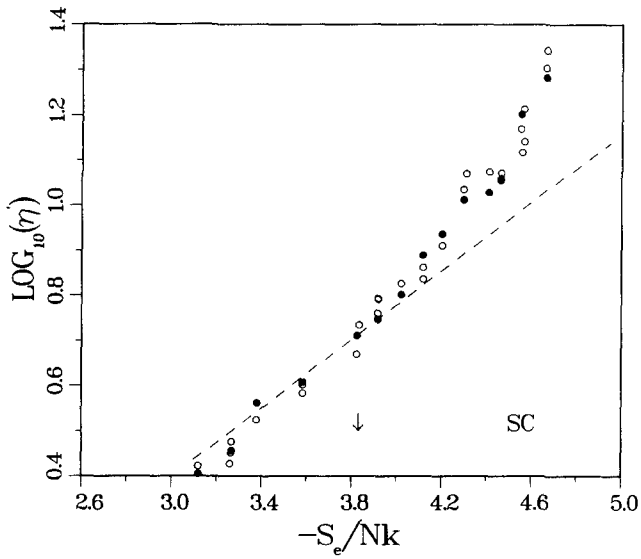

FIG. 6. Plot of the logarithm of η' as function of excess entropy ($-S_e/Nk$). [The excess entropy has been determined, as function of ρ^*, using the fit to Monte Carlo data of Hansen (Ref. 19).] The dashed line denotes the fit to the data outside the supercooled region given in Ref. 17. (Arrow indicates limit of supercooled.)

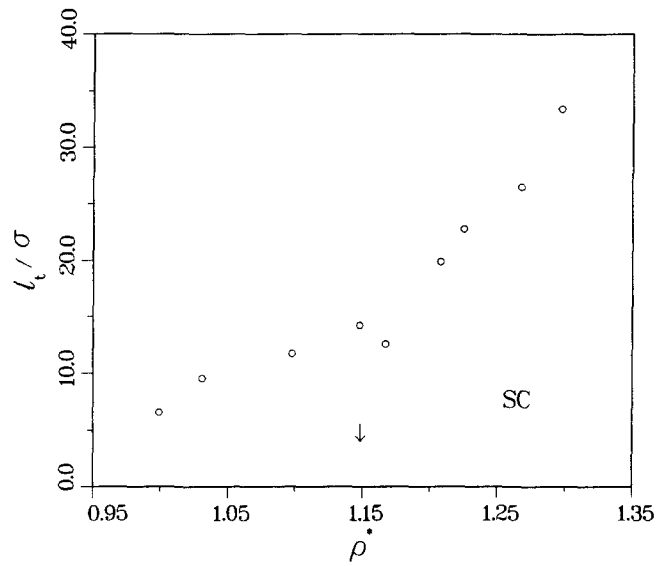

FIG. 7. Hydrodynamic length l_t [as obtained from Eq. (5)] vs ρ^*.

roughly the expression $\rho^{*(1/3)}/\tilde{\eta}^* = A(V^* - V_0^*)$, where $V^* = 1/\rho^*$ and V_0^* is a constant. Similarly, we note that the product $D\ \eta/\rho^{1/3}kT$ ($= \tilde{D}^*\tilde{\eta}^*/\rho^{*1/3}$) remained fairly constant throughout the supercooled region (i.e., $D\ \eta/\rho^{1/3}\ kT \simeq 0.148 \pm 0.017$). This is consistent with Stokes–Einstein behavior. These two results are consistent with the linear behavior of $\tilde{D}^*$ vs $1/\rho^*$ in the range $0.70 < \rho^* < 1.4$ previously observed by Cape and Woodcock.[5]

For completeness we note that, as previously observed,[7] the Enskog theory gives values for the shear viscosity which are too low near freezing. For comparison, the Enskog values for the reduced shear viscosity $\eta_E^*(\eta_E^* = \eta_E/\epsilon\tau\sigma^5\rho^{(8/3)})$ are plotted (calculated as in Ref. 7) also in Fig. 1. We note that the Enskog values remain relatively constant as a function of ρ^*.

We have also plotted the logarithm of the reduced viscosity η' [$\eta' = (\sigma/\epsilon\tau)\ \eta/\rho^{(2/3)}T^{*(1/2)}$] vs the excess entropy ($-S_e/Nk$), in order to compare with the work of Rosenfeld[16] and Grover, Hoover, and Moran.[17] These authors found that, when η' was plotted as a function of excess entropy for a $1/r^n$ potential for different values of n over a wide range of densities, the data all lay fairly close to a universal curve. We note that our data (Fig. 6) outside the supercooled region agrees approximately with the linear fit given by Grover, Hoover, and Moran in Ref. 17 for the $1/r^{12}$ potential. However, in the supercooled region, we find that the data deviate from this line—again indicating an enhancement in the viscosity.

B. Transverse-current correlation function

In addition to calculating the shear and bulk viscosity we have also calculated the transverse-current correlation function from the transverse-current density during the course of a run—where the transverse-current density was taken to be

$$J_T(k,t) = (1/N)\sum_{i=1}^{N} v_i^T(t)\exp[i\,\mathbf{k}\cdot\mathbf{r}_i(t)], \tag{4}$$

where v_i^T is that part of $\mathbf{v}_i$ which is perpendicular to $\mathbf{k}$ and the Cartesian components of the wave vector $\mathbf{k}$ are of the form

$$k_n = 2\pi n/L,$$

where n is an integer in order to satisfy periodic boundary conditions. The transverse-current correlation function is then

$$C_T(k,t) = \langle J_T(k,0)J_T(-k,t)\rangle. \tag{5}$$

For these calculations, the wave vectors were chosen to lie along the x, y, and z edges of the cube with $n = 1,2,\ldots,10$. The results for the three directions were averaged, while the time origins were separated by $10\,\Delta t$. Performing the Fourier transform to $\tilde{C}_T(k,\omega)$, we obtained $\mathrm{Re}\,\tilde{C}_T(k,\omega)$ as a function of ω for k_n, $n = 1,10$. Plotting the frequency of the (secondary) maximum as a function of k and extrapolating to the zero frequency intercept k_t gives a hydrodynamic length $l_t = 2\pi/k_t$ which is a measure[18] of the spatial extent of transverse dynamical correlations. This length is shown for several values of ρ^* in Fig. 7. We see that, along with the previously noted abrupt increase in the lifetime of the shear viscosity correlation function there is also a substantial increase in the hydrodynamic length l_t beyond the size of the box. This is consistent with results obtained previously for a model of liquid rubidium.[1]

As an independent check of our shear viscosity results, we have also used the transverse correlation function to calculate the wave-vector dependent, zero frequency shear viscosity $\eta^*(k)$ using

$$\eta(k) = \rho C_T(k,0)/[k^2\tilde{C}_T(k,0)] \tag{6}$$

and $\eta^*(k) = \eta(k)/\epsilon\tau\sigma^5\rho^{(8/3)}$ for $k = k_n$, $n = 1,10$. Figure 8 shows values of $\eta^*(k)$ for five different reduced densities along with the extrapolated values for $\eta^*(0)$. We note that for the two lowest values of ρ^* (0.9993 and 1.148) the value

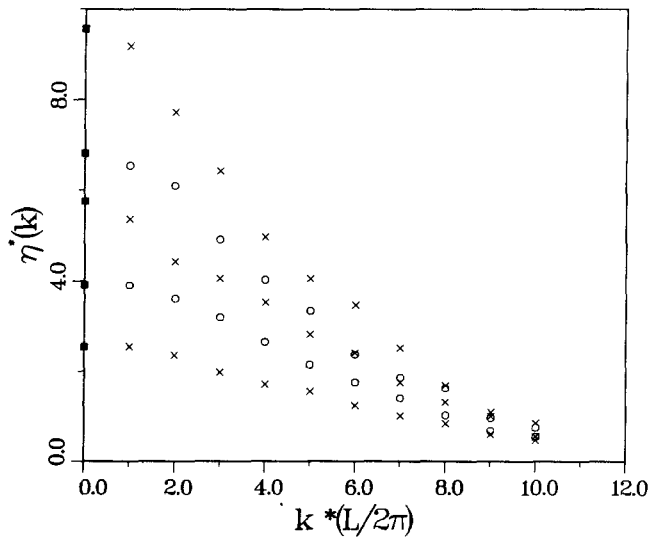

FIG. 8. $\eta^*(k_n)$, $n = 1,10$ for five different values of ρ^*. Going from bottom to top, they are $\rho^* = 0.999$, 1.148, 1.225, 1.268, 1.297. The dark squares correspond to $\eta^*(k = 0)$ values (extrapolated by eye).

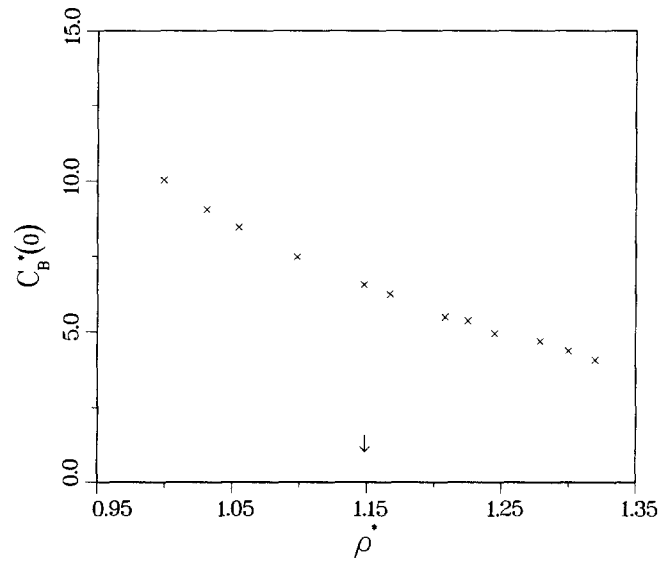

FIG. 10. (Similar to Fig. 2) Plot showing decrease of $C_B^*(0)$ with increasing ρ^*.

of $\eta^*(k_n, n = 1)$ appears to be indistinguishable from the asymptotic value $\eta^*(k = 0)$. This is consistent with the behavior of l_t which remains near or somewhat less than the box width L in this region. However for $\rho^* > 1.148$, $\eta^*(k)$ changes more rapidly with k (for small k), as expected, since l_t is significantly larger than the box width in this region. Figure 1 shows the extrapolated values of $\eta^*(k)$ as k goes to zero along with results obtained in the previous section. There is reasonably good agreement between the two results.

C. Bulk viscosity

Figure 9 shows our results for the reduced bulk viscosity $\eta_B^* = \eta_B/\epsilon\tau^2\sigma^5\rho^{(8/3)}$ as a function of reduced density ρ^*. This quantity remains virtually constant up until $\rho^* \simeq 1.15$ at which point it shows an abrupt change of slope as indicated by the dashed line in Fig. 9. Since the initial value of the correlation function $C_B^*(0)$ decreases steadily with increasing ρ^* (i.e., pressure fluctuations decrease as shown in Fig. 10), the abrupt increase in η_B^* is due to the development of a secondary tail in the pressure–pressure correlation function $C_B^*(t)$ which increases noticeably in the supercooled region. Figure 11 illustrates the development of this tail as the supercooled region is entered, while Fig. 12 shows more quantitatively the abrupt increase in its length in the supercooled region. We note that although this secondary tail increases in the supercooled region, the time at which $C_B^*(t)$ *first* crosses zero does not increase appreciably (from 0.06τ to about

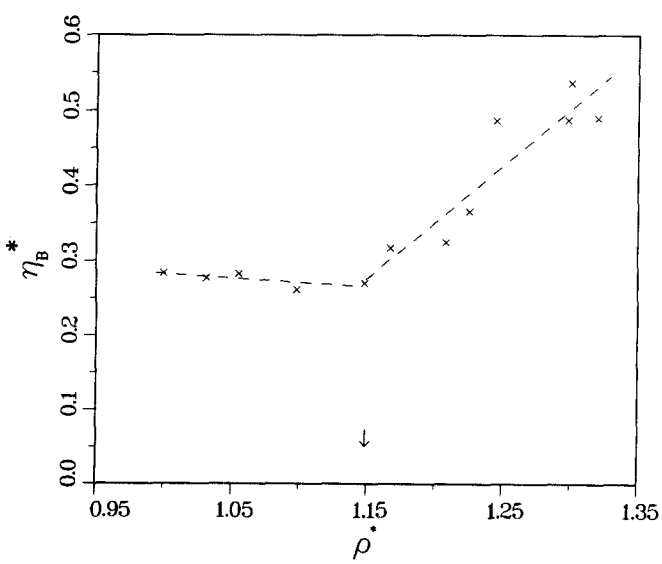

FIG. 9. Plot showing rapid increase in η_B^* as one enters the supercooled region (arrow indicates limit of supercooled). Dashed lines are merely to guide the eye.

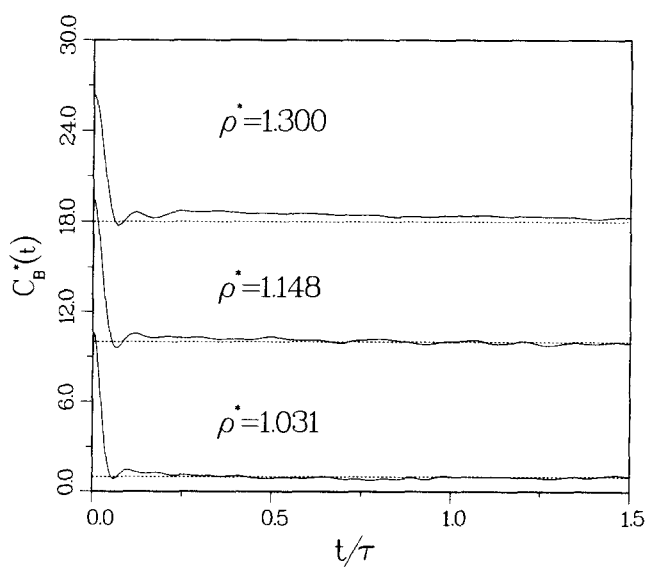

FIG. 11. Plot showing the growth of the tail of the time correlation function $C_B^*(t)$ with increasing ρ^*. For clarity, the correlation functions have been shifted upwards by 1, 9, and 18 units, respectively. (Dashed lines indicate zeroes of correlation function.)

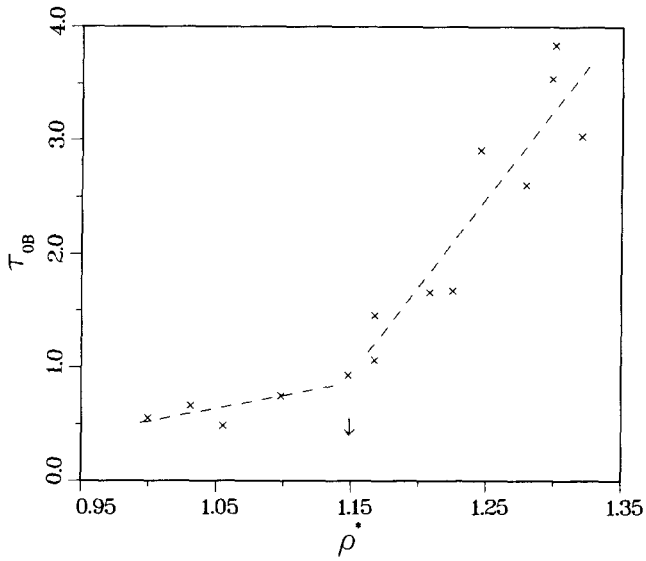

FIG. 12. Plot of τ_{0B}—the time for the tail of the correlation function $C_B^*(t)$ to reach zero (within statistical noise)—as a function of increasing ρ^*. Arrow indicates limit of supercooled. Dashed lines serve merely to guide the eye.

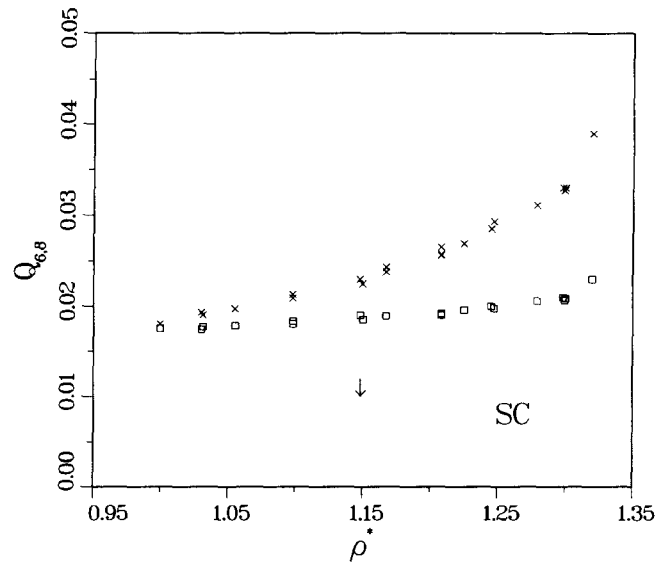

FIG. 13. Plot of Q_6 order parameter (crosses) and Q_8 (squares) as a function of ρ^*.

0.08τ, i.e., by about 30%) as one goes from the freezing temperature to the limit of supercooling. Thus, the enhancement of the bulk viscosity in the supercooled region is essentially due to this secondary tail.

We note that the calculation of the bulk viscosity from fluctuations is inherently more susceptible to statistical error than shear viscosity. This is due in part to the necessity of subtracting properly the average pressure (which may wander somewhat in the course of a run) in calculating the correlation function $C_B(t)$. As a result, we performed our calculation by subtracting a running average pressure ($\langle P \rangle$) taken over the last 1200 steps. Even so, we noticed a slight wandering of the long time behavior of our correlation function *away* (about 5% of the peak value) from zero for those runs done with strong supercooling. Thus, our results are expected to be somewhat more uncertain ($\pm$ 10%) in this region.

D. Thermal conductivity

The reduced thermal conductivity $\lambda_E^* = (\tau/k\sigma^7)\lambda_E/\rho^{(8/3)}$ was also calculated using Eq. (3). As previously mentioned, no significant change in either the thermal conductivity or the lifetime of the associated correlation function $C_E(t)$ was observed in the supercooled region.

We note that this behavior is in qualitative agreement with the results obtained from Enskog theory and in previous molecular dynamics simulations outside the supercooled region in which an increase of only a few percent in λ^* over a range of ρ^* from 1.0 to 1.15 was observed.[17]

E. Q_6 and Q_8 correlation functions

Steinhardt *et al.*[9] have shown that "bond-orientational order" can be significantly enhanced in the supercooled liquid. Figure 13 shows a plot of the bond-orientational order parameters Q_6 and Q_8, as a function of ρ^*, where Q_6 and Q_8 are defined by[9]

$$Q_l = \left\{ 4\pi/(2l+1) \sum_{m=-l}^{l} |\langle Y_{lm}(\mathbf{r}) \rangle|^2 \right\}^{1/2}.$$

The average $\langle Y_{lm}(\mathbf{r}) \rangle$ was taken over all nearest-neighbor pairs $\mathbf{r}_{ij}$ such that $|r_{ij}| < 1.4\sigma$ the first minimum in the pair correlation function $g(r)$. Values of Q_6 and Q_8 in the range 0–0.07 are characteristic of the disordered nature of a liquid, and values greater than 0.3 are characteristic of the fcc and bcc solids. Values in the intermediate range (0.15 ± 0.05) are characteristic of an amorphous solid or glass. As expected, Q_6 increases in the supercooled region but remains in the range of values characteristic of a liquid. On the other hand,

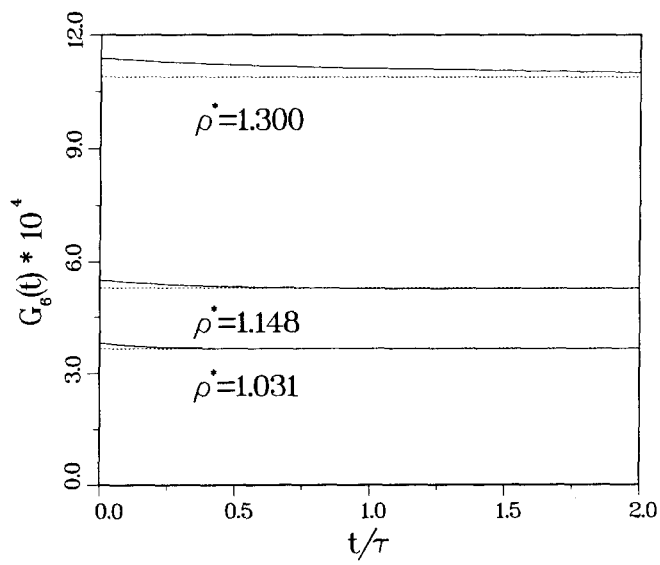

FIG. 14. Plot of $G_6(t)$ for three different values of ρ^*—showing development of tail with increasing ρ^*. (Dashed lines show long-time values of G_6 equal to $\langle Q_6 \rangle^2$.)

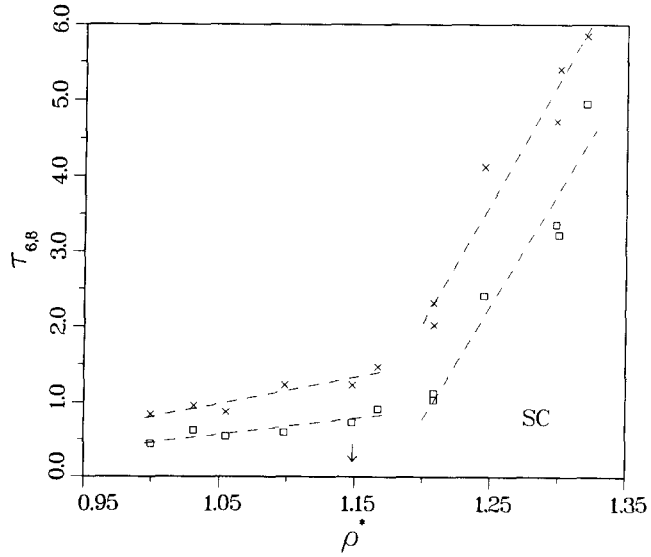

FIG. 15. Plot showing abrupt increase in the lifetimes τ_6 and τ_8 of correlation functions $G_6(t)$ and $G_8(t)$ in the supercooled region. (Dashed lines are merely guides to the eye.)

we note that Q_8 remains fairly constant throughout the supercooled region. We note at the same time that the magnitudes of the fluctuations in Q_6 and Q_8 remain quite small.

If, however, we look at the correlation functions $G_6(t) = \langle Q_6(0)Q_6(t)\rangle$ and $G_8(t) = \langle Q_8(0)Q_8(t)\rangle$, we see a marked increase in the *lifetime* of correlations as the supercooled region is entered (see Fig. 14). As a rough quantitative measure of this increase, we have plotted in Fig. 15 the times τ_6 and τ_8 for the correlation functions $G_6(t)$ and $G_8(t)$ to decay to their infinite-time values (within the statistical uncertainty) as a function of ρ^*. We note the "abrupt" change of slope upon entering the supercooled region. Thus, while the fluctuations of the local environment of a particle remain small in the supercooled region, the lifetime of these fluctuations appears to increase rapidly with degree of supercooling.

IV. DISCUSSION

Our results for the supercooled liquid state can be combined with other results (such as those of Ref. 5) to develop a picture of how the supercooled state differs from the equilibrium state for the $1/r^{12}$ fluid. The significant features appear to be those whose behavior changes abruptly as the supercooled state is entered. Among these are the time-correlation functions associated with fluctuations in the stress and in the local ordering of the neighborhood of a particle. Thus, for example, the diagonal components of the stress–stress time-correlation function, which correspond to the pressure–pressure correlation function, show an abrupt increase in the rate of change of lifetimes with increasing ρ^* as the supercooled region is entered. This is quantified by the rapid increase in the correlation time t_{0B} and in the bulk viscosity η_B^* (Figs. 9 and 11). Similarly, the off-diagonal components of the stress–stress time-correlation function, which correspond to the correlation function associated with the shear viscosity, show an abrupt change of behavior as the supercooled region is entered. This results in the enhancement of the shear viscosity in the supercooled region and the rapid increase of the correlation time τ_2 (Fig. 4). Finally, the lifetimes τ_6 and τ_8 of the order-parameter time-correlation functions $G_6(t)$ and $G_8(t)$ also show a fairly abrupt increase (Fig. 15) as the supercooled region is entered.

The behavior of these quantities is to be contrasted with the behavior of other quantities, studied here and in Ref. 5, which show a *smooth* behavior as the supercooled region is entered. These include thermodynamic equilibrium quantities (such as the specific heat and compressibility), equilibrium structural quantities such as the pair correlation function and the values of the Q_6 and Q_8 order parameters, and dynamic quantities such as the coefficient of diffusion, thermal conductivity, and the density–density time correlation function. The abrupt increase in the rate of change of the former quantities with increasing ρ^* as the supercooled region is entered, as well as the enhancement in the range l_t of transverse dynamical correlations observed for both supercooled liquid rubidium[1] and for the $1/r^{12}$ fluid, may in fact be features which distinguish the more general supercooled, metastable state from the thermodynamically stable liquid.

[1] R. D. Mountain, Phys. Rev. A **26**, 2859 (1982).
[2] W. G. Hoover, M. Ross, K. W. Johnson, D. Henderson, J. A. Barker, and B. C. Brown, J. Chem. Phys. **52**, 4931 (1970).
[3] W. G. Hoover, J. G. Gray, and K. W. Johnson, J. Chem. Phys. **55**, 1128 (1971).
[4] W. G. Hoover and M. Ross, Contemp. Phys. **12**, 339 (1971).
[5] J. N. Cape and L. V. Woodcock, J. Chem. Phys. **72**, 976 (1980).
[6] Y. Hiwatari, H. Matsuda, T. Ogawa, N. Ogita, and A. Ueda, Prog. Theor. Phys. **52**, 1105 (1974).
[7] W. T. Ashurst and W. G. Hoover, Phys. Rev. A **11**, 658 (1975).
[8] W. G. Hoover, A. J. C. Ladd, R. B. Hickman, and B. L. Holian, Phys. Rev. A **21**, 1756 (1980).
[9] P. J. Steinhardt, D. R. Nelson, and M. Ronchetti, Phys. Rev. Lett. **47**, 1297 (1981); Phys. Rev. B **28**, 784 (1983).
[10] D. Beeman, J. Comp. Phys. **20**, 130 (1976).
[11] A weak maximum in the pair-correlation function, at the position of the second neighbor distance, has been found to be a sensitive indication of short range fcc order. See H. J. Raveche, R. D. Mountain, and W. B. Streett, J. Chem. Phys. **61**, 1970 (1974).
[12] M. S. Green, J. Chem. Phys. **20**, 1281 (1952); **22**, 398 (1954).
[13] R. Kubo and K. Tomita, J. Phys. Soc. Jpn. **9**, 888 (1954).
[14] R. Zwanzig, Annu. Rev. Phys. Chem. **16**, 67 (1965).
[15] Note: In this paper we shall be dealing mainly with the reduced (dimensionless) quantities: the reduced shear viscosity ($\eta^* = \eta/\epsilon\tau\sigma^5\rho^{(8/3)}$), the reduced bulk viscosity ($\eta_B^* = \eta_B/\epsilon\tau\sigma^5\rho^{(8/3)}$), the reduced thermal conductivity [$\lambda_E^* = (\tau/k\sigma^7)\lambda_E/\rho^{(8/3)}$], and the reduced coefficient of diffusion [$D^* = (\tau/\sigma^7)D/\rho^{(5/3)}$] since these quantities depend only on a single thermodynamic variable—i.e., the reduced density ρ^*. One may also define the reduced viscosity $\tilde{\eta}^* = \eta^*\cdot\rho^{*(8/3)}$ and the reduced coefficient of diffusion $\tilde{D}^* = D^*\cdot\rho^{*(5/3)}$. See Ref. 6.
[16] Y. Rosenfeld, Phys. Rev. A **15**, 2545 (1977).
[17] R. Grover, W. G. Hoover, and B. Moran, J. Chem. Phys. **83**, 1255 (1985).
[18] G. Jacucci and I. R. McDonald, *Liquid & Amorphous Metals*, edited by E. Luscher and H. Coufal (Sijthoff & Noordhoff, Alphen aan den Rijn, The Netherlands, 1980), pp. 143–157.
[19] J. P. Hansen, Phys. Rev. A **2**, 221 (1970).